Multi-phase Synchronous Motors: Minimum Dissipation Fault-Tolerant Control with Currents Saturation

Marco Fei and Roberto Zanasi

***Abstract*— Multi-phase electrical motors offer high reliability thanks to their capability to operate safely even in case of faults such the loss of one or more phases. This paper deals with the control of multi-phase permanent magnet synchronous motors under open-phase faulty condition. Using a vectorial approach the optimal current references in faulty condition which provide the desired torque minimizing the dissipation and satisfying the limit current are obtained in the rotating reference frame. The approach is as general as possible: the proposed control law can be used for any shape of the rotor flux, for a generic odd number of phases and in presence of one or more phase failures.**

I. INTRODUCTION

In safety critical applications, i.e. propulsion and traction applications, the reliability is a very important issue. The most important advantage of multi-phase machines compared to three-phase one is the fault-tolerant capability of the motor drive: it can continue to operate with one or more failures (the theoretical maximum number of faults is m_s-3). In [1] and [2] a multi-phase synchronous motor is designed with a modular approach minimizing the electrical, magnetic and thermal coupling between the windings. Thus, a failure in one winding will not affect the operation of the remaining windings. However if the control is not modified the mean value of the torque decreases and a torque ripple appears. Several fault-tolerant controls have been proposed in the fixed reference frame [3]-[6] and in the rotating reference frame [7], [8].

In [3] the healthy-phase balanced currents are calculated keeping the magneto motive force (MMF) unchanged under the faults. Although a solution is obtained for a 5-phase synchronous motor where the 1-st and the 3-rd are injected, it is quite complex to generalize the proposed approach for machines with higher number of phases where the number of injected harmonics increases. Moreover this method does not minimize the global Joule losses and the torque ripple. In [4] the symmetry of the healthy-phase currents with respect to the location of the faulty phases is used reducing the torque pulsation and satisfying the star-connection constraint. An optimal solution is obtained for a 5-phase synchronous motor but also in this case the generalization of the control strategie is quite complex. In [5] the current vector in faulty conditions is obtained using the Lagrangian multipliers with the minimum dissipation function subject to the open phase and the minimum torque ripple constraints. Also in [6] a similar result is obtained with a different approach: the dimension of the *speed normalized back electromotive force* vector is adapted to the dimension of the remaining healthy-phases. These two methods hold for machines with a generic odd number of phases but the constraint on the maximum phase current limit is not taken into account. In [7] different control strategies are compared for a seven phase induction motor but it is not clear how the current references are obtained. In [8] a seven-phase synchronous motor with a particular shape of the rotor flux is used. Then the higher number of degrees of freedom of the drive is used in the post-fault strategie. Although this method is very interesting, it can be used only for a particular type of machines.

M. Fei and R. Zanasi are with the Information Engineering Department, University of Modena and Reggio Emilia, Via Vignolese 905, 41100 Modena, Italy, e-mail: {marco.fei, roberto.zanasi}@unimore.it.

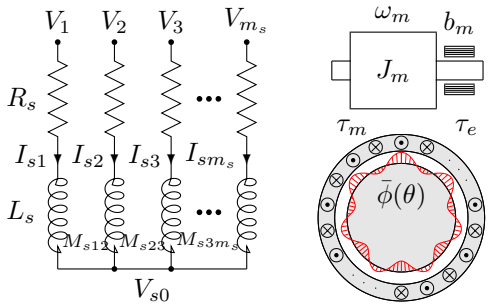

Fig. 1. Basic structure of a multi-phase synchronous motor.

In this paper the optimal fault-tolerant control strategie for multi-phase PM machine is studied in the rotating reference frame where it is easier to take into account the maximum phase current limit. Using a vectorial notation the proposed control law minimizes the power dissipation and the torque ripple. Moreover the post-fault strategie can be used for any shape of the rotor flux, for a generic odd number of phases and it works in presence of one or more open circuited failures.

The paper is organized as follows. Sec. II shows the details of the dynamic model of the m_s-phase synchronous motors, in Sec. III the control of the motor in open phase fault condition is presented and Sec. IV considers the maximum phase current limit. Some simulation results are presented in Sec. V and conclusions are given in Sec. VI.

A. Notations

The symbol $\sum_{n=a:d}^{b} c_n = c_a + c_{a+d} + c_{a+2d} + \dots$ will be used to represent the sum of a succession of numbers c_n where the index n ranges from a to b with increment d. The symbols $\mathbf{1}^m$ and $\mathbf{0}^m$ will represent ones and zeros column vectors of dimension m. Symbols $\text{Im}(\mathbf{A})$ and $\text{Ker}(\mathbf{A})$ will

denote the image and the kernel subspaces of matrix $\mathbf{A}$. The symbols $\overset{i}{\underset{1:n}{\left\|\left[\ R_i\ \right]\right\|}}$ and $\overset{i}{\underset{1:n}{\left\|\left[\ R_i\ \right]\right\|}}$ will denote the column and row matrices, while the full matrix will be denoted as:

$$\overset{i}{\underset{1:n}{\left\|\left[\ R_{i,j}\ \right]\right\|}}\overset{j}{\underset{1:m}{}} = \begin{bmatrix} R_{11} & R_{12} & \cdots & R_{1m} \\ R_{21} & R_{22} & \cdots & R_{2m} \\ \vdots & \vdots & \ddots & \vdots \\ R_{n1} & R_{n2} & \cdots & R_{nm} \end{bmatrix}.$$

II. ELECTRICAL MOTORS MODELING

The basic structure of a permanent magnet synchronous motor with an *odd* number m_s of concentrated winding in star connection is shown in Fig. 1 and its parameters are shown in Tab. I. The assumptions of regularity of the design, no reluctance effect and no iron saturation will be considered in this analysis. The dynamic model S_t of the multi-phase electrical motor can be expressed in the fixed frame Σ_t as:

$$\left[\begin{array}{c|c} {}^t\mathbf{L}_s & \mathbf{0} \\ \hline \mathbf{0} & J_m \end{array}\right]\left[\begin{array}{c} {}^t\dot{\mathbf{I}}_s \\ \hline \dot{\omega}_m \end{array}\right] = -\left[\begin{array}{c|c} {}^t\mathbf{R}_s & {}^t\mathbf{K}_\tau(\theta) \\ \hline -{}^t\mathbf{K}_\tau^{\mathrm{T}}(\theta) & b_m \end{array}\right]\left[\begin{array}{c} {}^t\mathbf{I}_s \\ \hline \omega_m \end{array}\right] + \left[\begin{array}{c} {}^t\mathbf{V}_s \\ \hline -\tau_e \end{array}\right] \quad (1)$$

where ${}^t\mathbf{V}_s$ and ${}^t\mathbf{I}_s$ are the voltage and the current stator vectors, while ${}^t\mathbf{R}_s$ and ${}^t\mathbf{L}_s$ are the resistance and the inductance matrices, respectively. The torque vector ${}^t\mathbf{K}_\tau(\theta)$ (also known as *speed normalized back electromotive force*) is function of the electric angle θ and the coefficients a_n of the rotor flux Fourier series shown in Tab. I. Note that according to the magnetic co-energy method the motor torque τ_m and the back-electromotive force vector ${}^t\mathbf{E}_s$ can be written as: $\tau_m = {}^t\mathbf{K}_\tau^{\mathrm{T}}\,{}^t\mathbf{I}_s$ and ${}^t\mathbf{E}_s = {}^t\mathbf{K}_\tau\omega_m$.

Applying to system S_t in (1) the following transformation matrix ${}^t\mathbf{T}_\omega \in \mathbb{R}^{m_s\times(m_s-1)}$, see [11]:

$${}^\omega\mathbf{T}_t = {}^t\mathbf{T}_\omega^{\mathrm{T}} = \sqrt{\frac{2}{m_s}}\overset{k}{\underset{1:2:m_s-2}{\left\|\left[\begin{array}{c}\cos(k((h-1)\gamma_s-\theta))\\ \sin(k((h-1)\gamma_s-\theta))\end{array}\right]\right\|}}\overset{h}{\underset{1:m_s}{}}. \quad (2)$$

one obtains a transformed and reduced system S_ω in the rotating frame Σ_ω:

$$\left[\begin{array}{c|c} {}^\omega\mathbf{L}_s & \mathbf{0} \\ \hline \mathbf{0} & J_m \end{array}\right]\left[\begin{array}{c} {}^\omega\dot{\mathbf{I}}_s \\ \hline \dot{\omega}_m \end{array}\right] = -\left[\begin{array}{c|c} {}^\omega\mathbf{R}_s + {}^\omega\mathbf{L}_s\,{}^\omega\mathbf{J}_s & {}^\omega\mathbf{K}_\tau(\theta) \\ \hline -{}^\omega\mathbf{K}_\tau^{\mathrm{T}}(\theta) & b_m \end{array}\right]\left[\begin{array}{c} {}^\omega\mathbf{I}_s \\ \hline \omega_m \end{array}\right] + \left[\begin{array}{c} {}^\omega\mathbf{V}_s \\ \hline -\tau_e \end{array}\right]. \quad (3)$$

In this rotating frame the m_s-phase motor can be seen as a set of $(m_s-1)/2$ independent electrical machines, rotating at different velocity $kp\omega_m$, each one working within a subspace $\Sigma_{\omega k}$ with $k \in \{1:2:m_s-2\}$.

The inductance and resistance transformed matrices ${}^\omega\mathbf{L}_s = {}^t\mathbf{T}_\omega^{\mathrm{T}}\,{}^t\mathbf{L}_s\,{}^t\mathbf{T}_\omega$ and ${}^\omega\mathbf{R}_s = {}^t\mathbf{T}_\omega^{\mathrm{T}}\,{}^t\mathbf{R}_s\,{}^t\mathbf{T}_\omega$ are diagonal matrices, while the coupling transformed matrix ${}^\omega\mathbf{J}_s = {}^t\mathbf{T}_\omega^{\mathrm{T}}\,{}^t\dot{\mathbf{T}}_\omega$ is a square matrix. These matrices can be written in vectorial notation as:

$${}^\omega\mathbf{L}_s = \overset{k}{\underset{1:2:m_s-2}{\left\|\left[\begin{array}{cc} L_{sk} & 0 \\ 0 & L_{sk}\end{array}\right]\right\|}},\quad {}^\omega\mathbf{J}_s = \overset{k}{\underset{1:2:m_s-2}{\left\|\left[\begin{array}{cc} 0 & -k\,\omega \\ k\,\omega & 0\end{array}\right]\right\|}},\quad {}^\omega\mathbf{R}_s = \overset{i}{\underset{1:m_s-1}{\left\|\left[\ R_s\ \right]\right\|}}$$

Note that the dimension of this matrices is m_s-1 because the rectangular transformation matrix ${}^t\mathbf{T}_\omega$ reduces the dynamic dimension of the system S_t imposing the star-connection constraint.

m_s	number of motor phases
p	number of polar expansions
θ, θ_m	electric and rotor angular positions: $\theta = p\,\theta_m$
ω, ω_m	electric and rotor angular velocities: $\omega = p\,\omega_m$
R_s	i-th stator phase resistance
L_s	i-th stator phase self induction coefficient
M_{s0}	maximum value of the stator mutual inductance
J_m	rotor moment of inertia
b_m	rotor linear friction coefficient
τ_m	electromotive torque acting on the rotor
τ_e	external load torque acting on the rotor
γ_s	basic angular displacement ($\gamma_s = 2\pi/m_s$)
$\phi_c(\theta)$	total rotor flux chained with stator phase 1
φ_c	maximum value of function $\phi_c(\theta)$
$\bar{\phi}(\theta)$	normalized total rotor flux: $\bar{\phi}(\theta) = \dfrac{\phi_c(\theta)}{\varphi_c} = \sum_{n=1:2}^{\infty} a_n \cos(n\,\theta)$

TABLE I

MAIN PARAMETERS OF A MULTI-PHASE SYNCHRONOUS MOTOR.

Neglecting the harmonics a_k of the rotor flux function $\bar{\phi}(\theta)$ with order over m_s, see [9], the transformed torque vector ${}^\omega\mathbf{K}_\tau = {}^t\mathbf{T}_\omega^{\mathrm{T}}\,{}^t\mathbf{K}_\tau(\theta)$ is constant (i.e. it is not function of the electric angle θ) with the following structure:

$${}^\omega\mathbf{K}_\tau = \overset{k}{\underset{1:2:m_s-2}{\left\|\left[\ \overline{K}_{\tau k}\ \right]\right\|}} = \overset{k}{\underset{1:2:m_s-2}{\left\|\left[\begin{array}{c} K_{dk} \\ K_{qk}\end{array}\right]\right\|}} = p\,\varphi_c\sqrt{\frac{m_s}{2}}\overset{k}{\underset{1:2:m_s-2}{\left\|\left[\begin{array}{c} 0 \\ k\,a_k\end{array}\right]\right\|}}, \quad (4)$$

each component $\overline{K}_{\tau k}$ is defined by the coefficient a_n of the same order k. The motor torque τ_m and the transformed back-electromotive force vector ${}^\omega\mathbf{E}_s$ can be written as:

$$\tau_m = {}^\omega\mathbf{K}_\tau^{\mathrm{T}}\,{}^\omega\mathbf{I}_s\,, \qquad {}^\omega\mathbf{E}_s = {}^\omega\mathbf{K}_\tau\omega_m. \quad (5)$$

When the first $(m_s-1)/2$ odd harmonics are injected in the stator phases, the transformed current and voltage vectors ${}^\omega\mathbf{I}_s = {}^t\mathbf{T}_\omega^{\mathrm{T}}\,{}^t\mathbf{I}_s$ and ${}^\omega\mathbf{V}_s = {}^t\mathbf{T}_\omega^{\mathrm{T}}\,{}^t\mathbf{V}_s$ are:

$${}^\omega\mathbf{I}_s = \overset{k}{\underset{1:2:m_s-2}{\left\|\left[\ \overline{I}_{sk}\ \right]\right\|}} = \overset{k}{\underset{1:2:m_s-2}{\left\|\left[\begin{array}{c} I_{dk} \\ I_{qk}\end{array}\right]\right\|}},\quad {}^\omega\mathbf{V}_s = \overset{k}{\underset{1:2:m_s-2}{\left\|\left[\ \overline{V}_{sk}\ \right]\right\|}} = \overset{k}{\underset{1:2:m_s-2}{\left\|\left[\begin{array}{c} V_{dk} \\ V_{qk}\end{array}\right]\right\|}} \quad (6)$$

where each harmonic of order k and amplitude I_{mk} and V_{mk} is transformed into vectors $\overline{I}_{sk}$ and $\overline{V}_{sk}$ moving in the subspace $\Sigma_{\omega k}$. These vectors $\overline{I}_{sk}$ and $\overline{V}_{sk}$ are constant in steady-state condition and they are defined by the *direct* and *quadrature* components I_{dk}, I_{qk}, V_{dk} and V_{qk}, respectively. The modulus $|\overline{I}_{sk}|$ and $|\overline{V}_{sk}|$ are related to the amplitude I_{mk} and V_{mk} by the following relations:

$$|\overline{I}_{sk}| = \sqrt{I_{dk}^2 + I_{qk}^2} = \sqrt{\frac{m_s}{2}}\;I_{mk} \quad (7)$$

$$|\overline{V}_{sk}| = \sqrt{V_{dk}^2 + V_{qk}^2} = \sqrt{\frac{m_s}{2}}\;V_{mk} \quad (8)$$

Using the Power-Oriented Graphs modeling technique, see [10], one obtains the POG block scheme of the synchronous motor in the rotating reference frame Σ_ω shown in Fig. 2.

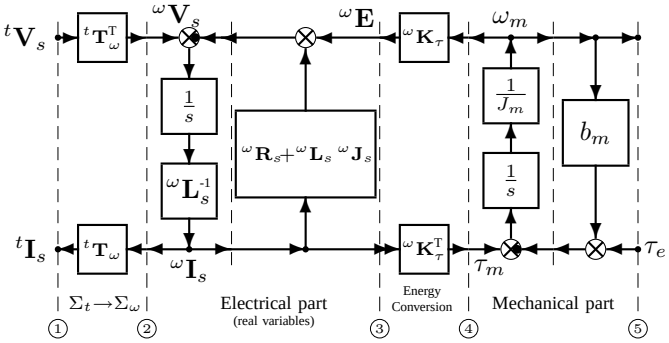

Fig. 2. POG block scheme of a multi-phase synchronous motor in the rotating frame Σ_ω.

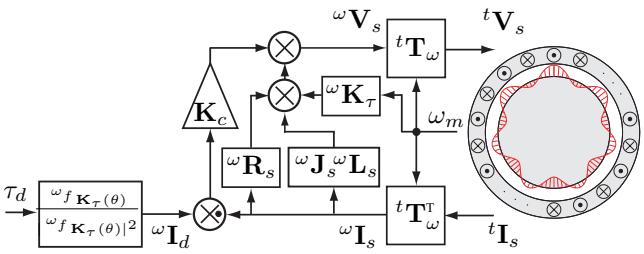

Fig. 3. Multi-phase control motor drive scheme in healthy condition in the rotating reference frame.

The *connection block* between sections ①-② represents the state space transformation ${}^t\mathbf{T}_\omega$ between the fixed reference frame Σ_t and the rotating reference frame Σ_ω. The *elaboration blocks* between the power sections ②-③ represent the *Electrical part* of the system, while the blocks between sections ④-⑤ represent the *Mechanical part* of the system. The *connection block* between sections ③-④ represents the energy and power conversion (without accumulation nor dissipation) between the electrical and mechanical parts of the motor.

III. Minimum dissipation torque control in the rotating reference frame

A. Control in healthy condition

Since in (5) the motor torque τ_m is obtained as the scalar product between the transformed torque and current vectors ${}^\omega\mathbf{K}_\tau$ and ${}^\omega\mathbf{I}_s$, then the desired current vector ${}^\omega\mathbf{I}_d$ which provides the desired torque τ_d minimizing the power dissipation is the vector with the minimum modulus parallel to the transformed torque vector ${}^\omega\mathbf{K}_\tau$:

$$ {}^\omega\mathbf{I}_d = \frac{{}^\omega\mathbf{K}_\tau}{|{}^\omega\mathbf{K}_\tau|^2}\,\tau_d = \left\| \begin{bmatrix} 0 \\ \widetilde{K}_k \end{bmatrix} \right\|_{1:2:m_s-2}^{k} \tau_d\,, \qquad \widetilde{K}_k = \frac{K_{qk}}{|{}^\omega\mathbf{K}_\tau|^2}. \tag{9} $$

where the distribution coefficients $\widetilde{K}_k$ relate the modulus $|\overline{I}_{sk}|$ with the harmonic spectrum of the rotor flux.
The desired constant torque can be reached using equation (9) in the following control law:

$$ {}^\omega\mathbf{V}_s = ({}^\omega\mathbf{R}_s + {}^\omega\mathbf{J}_s\,{}^\omega\mathbf{L}_s)\,{}^\omega\mathbf{I}_s + {}^\omega\mathbf{K}_\tau\,\omega_m - \mathbf{K}_c({}^\omega\mathbf{I}_s - {}^\omega\mathbf{I}_d) \tag{10} $$

where feed-forward action and a P controller are used. The equations (9) and (10) are used together in the control block diagram shown in Fig. 3. Using this control the first odd harmonics of order below m_s are injected increasing the torque production capability of the machines. Moreover the harmonic spectrum of the current is tied to the harmonic spectrum of the rotor flux.

B. Control in faulty condition

Assuming the failures do no affect the operation of the remaining healthy windings; when f open-phase faults occur the related phase currents fall down to zero and they do not contribute any more to the torque generation . In this case the open phase constraints can be taken into account projecting the transformed torque vector onto the $m_s - f$ dimensional subspace generated by the healthy currents.
Let $\mathcal{S} = \{i_1, i_2, ..., i_f\}$ denote the index set of the faulty phases with $f \leq m_s - 3$, the open phase constraints can be written as:

$$ {}^t\mathbf{B}^{\mathrm{T}}\,{}^t\mathbf{I}_s = \left[I_{si_1}\,,\, I_{si_2}\,, \cdots, I_{si_f}\right]^{\mathrm{T}} = (\mathbf{0}^f)^{\mathrm{T}} $$

where the matrix ${}^t\mathbf{B}$ is defined as:

$$ {}^t\mathbf{B} = [\mathbf{e}_{i_1}^{m_s}\ \mathbf{e}_{i_2}^{m_s}\ \cdots\ \mathbf{e}_{i_f}^{m_s}] \tag{11} $$

Note that the i-th standard basis vector $\mathbf{e}_i^{m_s}$ of space $\mathbb{R}^{m_s}$ is used to select the i-th fault component I_{si} of the current vector ${}^t\mathbf{I}_s$. Therefore the vectors $\mathbf{e}_{i_1}^{m_s}$, $\mathbf{e}_{i_2}^{m_s}$, $\cdots$ and $\mathbf{e}_{i_f}^{m_s}$ form a basis of the f-dimensional forbidden subspace $\mathrm{Im}({}^t\mathbf{B})$ in the fixed reference frame.
Since the transformed current vector is ${}^\omega\mathbf{I}_s = {}^t\mathbf{T}_\omega^{\mathrm{T}}\,{}^t\mathbf{I}_s$, then the open phase constraint can be written as:

$$ {}^t\mathbf{B}^{\mathrm{T}}\,{}^t\mathbf{I}_s = {}^t\mathbf{B}^{\mathrm{T}}\,{}^t\mathbf{T}_\omega\,{}^\omega\mathbf{I}_s = {}^\omega\mathbf{B}^{\mathrm{T}}\,{}^\omega\mathbf{I}_s = (\mathbf{0}^f)^{\mathrm{T}} $$

where the constraint matrix ${}^\omega\mathbf{B}$ in the rotating reference frame is defined as:

$$ {}^\omega\mathbf{B} = ({}^t\mathbf{B}^{\mathrm{T}}\,{}^t\mathbf{T}_\omega)^{\mathrm{T}} = {}^t\mathbf{T}_\omega^{\mathrm{T}}\,{}^t\mathbf{B} = {}^\omega\mathbf{T}_t\,{}^t\mathbf{B}. \tag{12} $$

Substituting (2) and (11) in (12) one obtains:

$$ {}^\omega\mathbf{B} = \left\| \begin{bmatrix} \cos(k((h-1)\gamma_s - \theta)) \\ \sin(k((h-1)\gamma_s - \theta)) \end{bmatrix} \right\|_{1:2:m_s-2}^{h\,\in\,\mathcal{S}} = \left[\mathbf{w}_{i_1}\,\mathbf{w}_{i_2}\,\cdots\,\mathbf{w}_{i_f}\right], $$

where the vectors $\mathbf{w}_{i_1}$, $\mathbf{w}_{i_2}$, $\cdots$ and $\mathbf{w}_{i_f}$ (that are the columns of the transformation ${}^\omega\mathbf{T}_t$ related to the faulty phases) form a basis of the f-dimensional forbidden subspace $\mathrm{Im}({}^\omega\mathbf{B})$ in the rotating reference frame.
The subspace $\mathrm{Ker}({}^\omega\mathbf{B}^{\mathrm{T}})$, which is orthogonal to the forbidden subspace $\mathrm{Im}({}^\omega\mathbf{B})$, is the subspace of the healthy currents that satisfies the constraints. Therefore the current constraints are satisfied if the transformed torque vector ${}^\omega\mathbf{K}_\tau$ is projected on $\mathrm{Ker}({}^\omega\mathbf{B}^{\mathrm{T}})$ along $\mathrm{Im}({}^\omega\mathbf{B})$. The projection matrix ${}^\omega\mathbf{P}$ on $\mathrm{Ker}({}^\omega\mathbf{B}^{\mathrm{T}})$ along $\mathrm{Im}({}^\omega\mathbf{B})$ is defined as follows:

$$ {}^\omega\mathbf{P} = \mathbf{I}_{m_s-1} - {}^\omega\mathbf{B}\left({}^\omega\mathbf{B}^{\mathrm{T}}\,{}^\omega\mathbf{B}\right)^{-1}{}^\omega\mathbf{B}^{\mathrm{T}}. $$

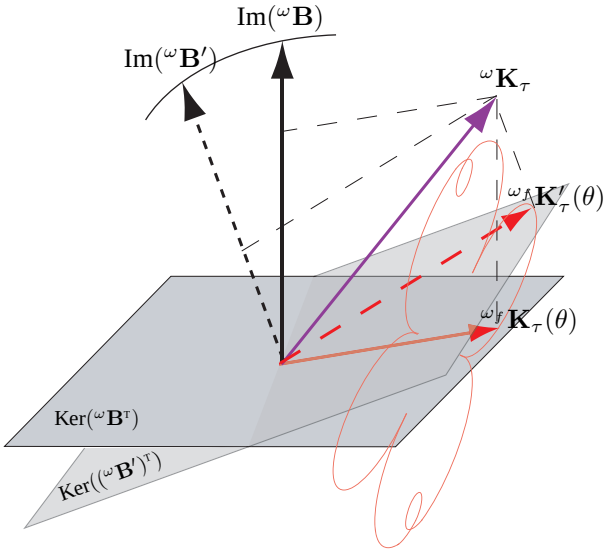

Fig. 4. Projection of a torque vector onto the subspace of healthy currents.

Using this projection matrix ${}^{\omega}\mathbf{P}$ one can obtain the following projected torque vector ${}^{\omega_f}\mathbf{K}_\tau(\theta)$:

$$ {}^{\omega_f}\mathbf{K}_\tau(\theta) = {}^{\omega}\mathbf{P}\,{}^{\omega}\mathbf{K}_\tau = \left\| \begin{bmatrix} {}^{f}K_{dk}(\theta) \\ {}^{f}K_{qk}(\theta) \end{bmatrix} \right\|_{1:2:m_s-2}^{k}. \tag{13} $$

Note that the vectors $\mathbf{w}_{i_1}$, $\mathbf{w}_{i_2}$ $\cdots$ and $\mathbf{w}_{i_f}$ are function of the electric angle θ, then also the forbidden subspace $\mathrm{Im}({}^{\omega}\mathbf{B})$ is function of θ. Consequently the projected torque vector ${}^{\omega_f}\mathbf{K}_\tau(\theta)$ is a periodic function of the electric angle θ.

A graphical representation of equation (13) at two different time t' and t, with $t' < t$, is shown in Fig. 4: the transformed torque vector ${}^{\omega}\mathbf{K}_\tau(\theta)$ (the violet vector) is constant while the forbidden subspace $\mathrm{Im}({}^{\omega}\mathbf{B})$ (the black vector) is function of the electric angle θ. Note that the variation of the forbidden subspace from $\mathrm{Im}({}^{\omega}\mathbf{B}')$ to $\mathrm{Im}({}^{\omega}\mathbf{B})$ modifies from $\mathrm{Ker}({}^{\omega}\mathbf{B}'^{\mathrm{T}})$ to $\mathrm{Ker}({}^{\omega}\mathbf{B}^{\mathrm{T}})$ the subspace of the healthy currents satisfying the fault constraints. In Fig. 4, the projection of the transformed torque vector ${}^{\omega_f}\mathbf{K}_\tau(\theta)$ (the red vector) is a periodic function of the electric angle and it describes a periodic trajectory (the red line).

Substituting equation (13) in (9) one obtains the desired current vector ${}^{\omega_f}\mathbf{I}_d$ in frame Σ_ω under fault condition which provides the desired torque τ_d minimizing the power dissipation:

$$ {}^{\omega_f}\mathbf{I}_d(\theta) = \frac{{}^{\omega_f}\mathbf{K}_\tau(\theta)}{|{}^{\omega_f}\mathbf{K}_\tau(\theta)|^2}\,\tau_d = \left\| \begin{bmatrix} {}^{f}I_{dk}(\theta) \\ {}^{f}I_{qk}(\theta) \end{bmatrix} \right\|_{1:2:m_s-2}^{k}, \tag{14} $$

where the direct ${}^{f}I_{dk}$ and quadrature ${}^{f}I_{qk}$ are:

$$ {}^{f}I_{dk}(\theta) = \frac{{}^{f}K_{dk}(\theta)}{|{}^{\omega_f}\mathbf{K}_\tau(\theta)|^2}\,\tau_d\,, \quad {}^{f}I_{qk}(\theta) = \frac{{}^{f}K_{qk}(\theta)}{|{}^{\omega_f}\mathbf{K}_\tau(\theta)|^2}\,\tau_d. \tag{15} $$

The direct component ${}^{f}I_{dk}$ of the current vectors $\overline{I}_{sk}$ must be used to satisfy the faulty constraint despite they dissipate power without producing torque (in (4) the direct components K_{dk} of the torque vectors $\overline{K}_{\tau k}$ are zero).

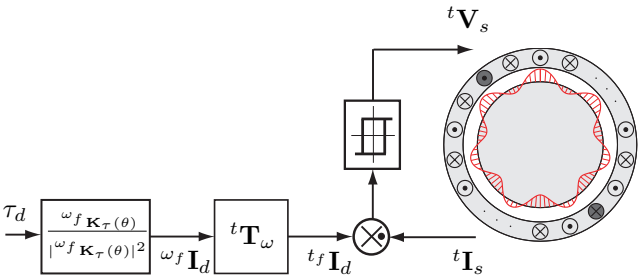

Fig. 5. Multi-phase control motor drive under fault condition.

The condition ${}^{\omega}\mathbf{I}_s = {}^{\omega_f}\mathbf{I}_d$ can not be achieved using the control law (10) because the desired current is a periodic function of the electric angle θ. Therefore an undesired torque ripple (due to the tacking error) appears if the block diagram shown in Fig. 3 is used. This problem can be overcome transforming the desired current vector ${}^{\omega_f}\mathbf{I}_d$ in the rotating reference frame to the desired current vector ${}^{t_f}\mathbf{I}_d$ in the fixed reference frame as follows:

$$ {}^{t_f}\mathbf{I}_d(\theta) = {}^{t}\mathbf{T}_\omega\,{}^{\omega_f}\mathbf{I}_d(\theta). $$

Then an hysteresis current controller can be used in order to follow the time variant reference current vector ${}^{t_f}\mathbf{I}_d(\theta)$, see Fig. 5. Using the proposed control the multi-phase motor continues to operate safely (generating the same desired torque without ripple) under a phase-faults without any additional hardware connections.

IV. Current Limit

It is well known in the literature that fault-tolerant controls increase the current amplitude in the healthy phases. The main advantages of the proposed control respect to the others in [5] and [6] is that the maximum current limit can be taken into account. When the amplitudes of the components of the current vectors ${}^{t}\mathbf{I}_s$ are bounded by the the maximum rated current I_{max} the following constraint hold:

$$ \sum_{k=1:2}^{m_s-2} I_{mk} \le I_{max}. \tag{16} $$

Using (7) the constraint (16) can be rewritten as:

$$ \sum_{k=1:2}^{m_s-2} |\overline{I}_{sk}| \le \sqrt{\frac{m_s}{2}}\,I_{max}, \tag{17} $$

where the modulus of the current vectors I_{sk} is defined from (7) and (15) as:

$$ |\overline{I}_{sk}| = \sqrt{{}^{f}K_{dk}^2 + {}^{f}K_{qk}^2}\;\frac{\tau_d}{|{}^{\omega_f}\mathbf{K}_\tau(\theta)|^2}. \tag{18} $$

Substituting (18) in (17) one obtains the maximum torque in faulty condition minimizing the current dissipation and satisfying the maximum current limit I_{max}:

$$ \tau_c(\theta) = \frac{|{}^{\omega_f}\mathbf{K}_\tau(\theta)|^2}{\displaystyle\sum_{k=1:2}^{m_s-2} \sqrt{{}^{f}K_{dk}(\theta)^2 + {}^{f}K_{qk}(\theta)^2}}\sqrt{\frac{m_s}{2}}\,I_{max}. \tag{19} $$

Equation (19) transforms the current limit in a torque limit, so when $\tau_d > \tau_c(\theta)$ the desired torque is saturated to the maximum value satisfying the maximum current limit. Introducing (19) in (14) one obtains the desired current vector ${}^{\omega_f}\mathbf{I}_d$ in frame Σ_ω under fault condition minimizing the power dissipation and satisfying the current limit:

$$ {}^{\omega_f}\mathbf{I}_d(\theta) = \begin{cases} \dfrac{{}^{\omega_f}\mathbf{K}_\tau(\theta)}{|{}^{\omega_f}\mathbf{K}_\tau(\theta)|^2}\,\tau_d & \text{if} \quad \tau_d \le \tau_c(\theta) \\ \dfrac{{}^{\omega_f}\mathbf{K}_\tau(\theta)}{|{}^{\omega_f}\mathbf{K}_\tau(\theta)|^2}\,\tau_c(\theta) & \text{if} \quad \tau_d > \tau_c(\theta) \end{cases} \tag{20} $$

The dependence of τ_c from θ produces a time variant motor torque τ_m. In the applications where a constant torque is required it is necessary to compute the minimum of the maximum torque $\min(\tau_c(\theta))$. It can be made in the algorithm comparing the actual value $\tau_c(\theta)$ with the stored value τ_{cs} and saving the actual value in the stored value $\tau_{cs} = \tau_c(\theta)$ if $\tau_c(\theta) < \tau_{cs}$. Therefore after a period $T = 2\pi t/\theta$ one obtains the minimum value $\tau_{cs} = \min(\tau_c(\theta))$. In this case the current vector ${}^{\omega_f}\mathbf{I}_d$ is obtained as:

$$ {}^{\omega_f}\mathbf{I}_d(\theta) = \begin{cases} \dfrac{{}^{\omega_f}\mathbf{K}_\tau(\theta)}{|{}^{\omega_f}\mathbf{K}_\tau(\theta)|^2}\,\tau_d & \text{if} \quad \tau_d \le \tau_{cs} \\ \dfrac{{}^{\omega_f}\mathbf{K}_\tau(\theta)}{|{}^{\omega_f}\mathbf{K}_\tau(\theta)|^2}\,\tau_{cs} & \text{if} \quad \tau_d > \tau_{cs} \end{cases} \tag{21} $$

Note that there is a trade-off between the torque mean value and the torque ripple: the (20) provides an higher torque with ripple, while the (21) provides a lower torque without ripple.

V. Simulations

The simulation results shown in this section have been obtained in Matlab-Simulink using the POG model of the electrical motor in faulty condition described in [12] and characterized by the following electrical and mechanical parameters: $m_s = 5$, $p = 1$, $R_s = 2\,\Omega$, $L_s = 0.03$ H, $M_{s0} = 0.01$ H, $\varphi_r = 0.02$ Wb, $J_m = 1.6$ kg m^2, $b_m = 0.8$ Nm s/rad, $a_1 = 1$, $a_3 = 0.25$, $I_{max} = 30$ A, desired torque $\tau_d = 18$ Nm and no external torque $\tau_e = 0$ Nm.

The strategies (14), (20) and (21) are compared under two adjacent open-phase faults: the faults occur at times $t_1 = 1.5$ and $t_1 = 4$ on the 2-nd and the 3-rd phase, respectively; while the controls are activated at time $t_2 = 1.5$ s and at time $t_4 = 4.5$ s.

The motor velocity ω_m and the motor torque τ_m obtained using (14) are shown in Fig. 6. When the first open-phase fault occurs the mean value of the torque decreases and the torque ripple appears (between t_1 and t_2 the control is unchanged with respect to the healthy condition). At time t_2 when the fault tolerant control is applied the torque grows up to the desired value $\tau_m = \tau_d = 30$ Nm without ripple. When the second open-phase fault occurs the mean value of the torque decreases again and the torque ripple appears because between t_3 and t_4 there are two open phases but the control is not modified with respect to the first failure case. At time t_4 the fault tolerant control is applied and the

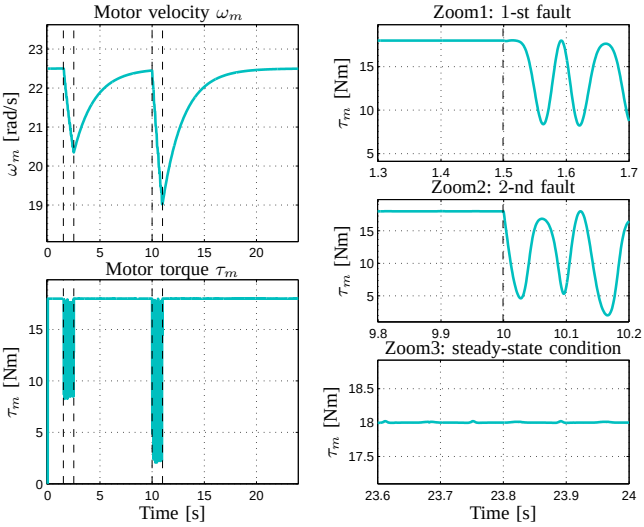

Fig. 6. Motor velocity ω_m and motor torque τ_m using control (14).

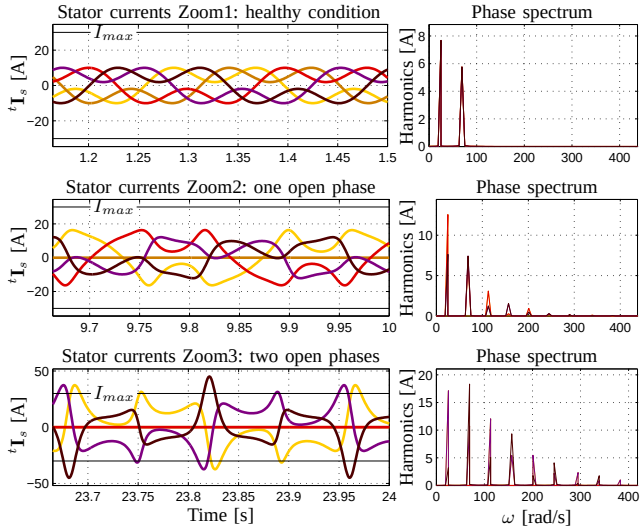

Fig. 7. Zoom of the stator current vector ${}^t\mathbf{I}_s$ in the fixed reference frame with its corresponding harmonic spectrum obtained using control (14) .

torque grows up to the desired value τ_d without ripple.

Fig. 7 shows the zooms of the stator current vectors ${}^t\mathbf{I}_s$ in the fixed reference frame with its corresponding spectrum in healthy condition and when the fault tolerant control is activated. In healthy condition only the 1-st and the 3-rd harmonics are injected, while when the post-fault control is activated more odd harmonics of higher order are injected. Using (14) the amplitude of the healthy phase currents increases and the maximum phase current limit I_{max} is not satisfied when the second fault occurs (this control does not take into account the maximum current constraint).

The motor velocity ω_m and the motor torque τ_m obtained using (20) and (21) are presented in Fig. 8, while the zooms of the stator current vectors ${}^t\mathbf{I}_s$ are shown in Fig. 9. At time t_2 when the saturated fault tolerant controls are applied the torque grows to a lower value of τ_d in order to satisfy the maximum phase current limit I_{max} (see Fig. 9). Using (20) one obtains a torque mean value of 17.03 Nm

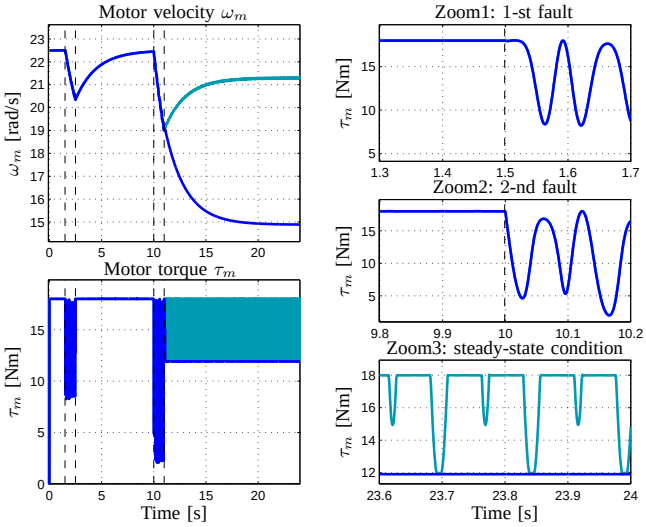

Fig. 8. Motor velocity ω_m and motor torque τ_m obtained using control (20) (teal) and control (21) (blue).

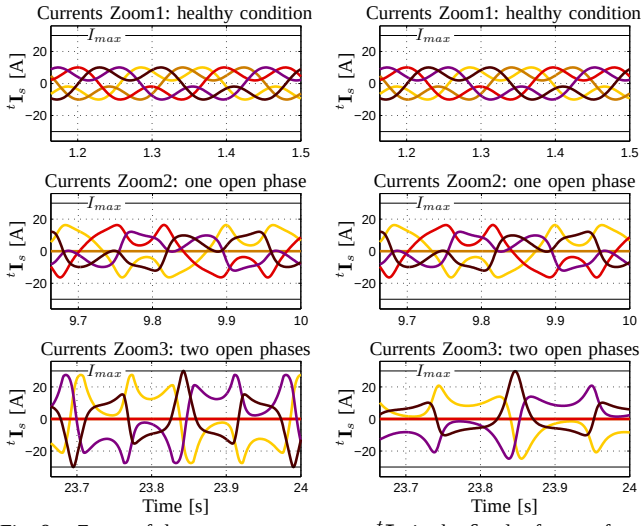

Fig. 9. Zoom of the stator current vector ${}^t\mathbf{I}_s$ in the fixed reference frame obtained using control (20) (on the left) and control (21) (on the right).

with ripple while using (21) one obtains a lower torque $\tau_m = \min(\tau_c(\theta)) = 11.8$ Nm without ripple. In Fig. 10 one can see the *direct* and *quadrature* components I_{dk}, I_{qk} in the rotating reference frame: they are constant in healthy condition while they are a periodic function of the electric angle θ in faulty condition. It is found that both the components oscillate at frequencies 2ω, 4ω, ... where $\omega = p\omega_m$.

VI. Conclusion

In this paper the control of multi-phase permanent magnet synchronous motors under open-phase fault condition has been investigated taking into account the maximum phase current limit. The proposed control laws minimize the power dissipation and the torque ripple. Moreover the post-fault strategies are suitable for motors with a generic number of phases and in presence of one or more phase failures.

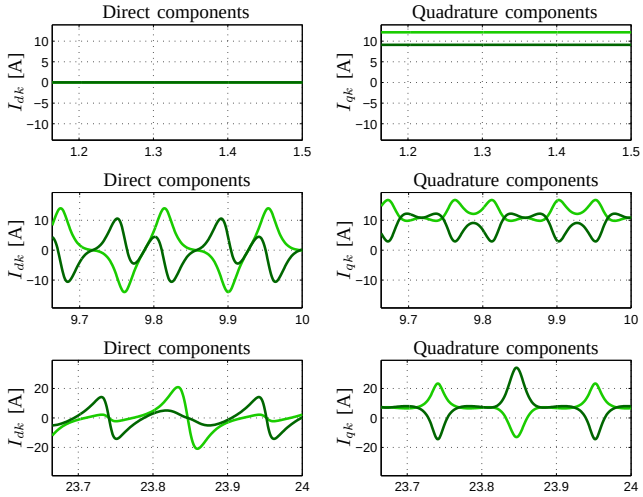

Fig. 10. Direct and quadrature components I_{dk}, I_{qk} in the rotating reference frame ($k = 1$ green, $k = 3$ dark green) obtained using control (21).

The use of the POG modeling technique allows a direct implementation of the control in Simulink. Some simulation results show the effectiveness of the proposed model in the case of two adjacent open phases of a 5-phase motor.

References

[1] Mecrow, B.C.; Jack, A.G.; Haylock, J.A.; Coles, J.; , "Fault-tolerant permanent magnet machine drives", Electric Power Applications, IEE Proceedings -, vol.143, no.6, pp.437-442, Nov 1996

[2] Abolhassani, M.T.; Toliyat, H.A.; , "Fault tolerant permanent magnet motor drives for electric vehicles", Electric Machines and Drives Conference, 2009. IEMDC '09.

[3] Bianchi, N.; Bolognani, S.; Pre, M.D.; , "Strategies for the Fault-Tolerant Current Control of a Five-Phase Permanent-Magnet Motor", IEEE Transactions on Industry Applications, vol.43, no.4, pp.960-970, July-aug. 2007

[4] Dwari, S.; Parsa, L.; , "Fault-Tolerant Control of Five-Phase Permanent-Magnet Motors With Trapezoidal Back EMF", IEEE Transactions on Industrial Electronics, vol.58, no.2, pp.476-485, Feb. 2011

[5] Dwari, S.; Parsa, L.; , "An Optimal Control Technique for Multiphase PM Machines Under Open-Circuit Faults", IEEE Transactions on Industrial Electronics, vol.55, no.5, pp.1988-1995, May 2008

[6] Kestelyn, X.; Semail, E.; , "A Vectorial Approach for Generation of Optimal Current References for Multiphase Permanent-Magnet Synchronous Machines in Real Time", IEEE Transactions on Industrial Electronics, vol.58, no.11, pp.5057-5065, Nov. 2011

[7] Tani, A.; Mengoni, M.; Zarri, L.; Serra, G.; Casadei, D.; , "Control of Multiphase Induction Motors With an Odd Number of Phases Under Open-Circuit Phase Faults", IEEE Transactions on Power Electronics, vol.27, no.2, pp.565-577, Feb. 2012

[8] Locment, F.; Semail, E.; Kestelyn, X.; , "Vectorial Approach-Based Control of a Seven-Phase Axial Flux Machine Designed for Fault Operation", IEEE Transactions on Industrial Electronics, vol.55, no.10, pp.3682-3691, Oct. 2008

[9] Zanasi, R.; Grossi, F.; , "Optimal Rotor Flux Shape for Multi-phase Permanent Magnet Synchronous Motors", International Power Electronics and Motion Control Conference, 2008, Poznan, Poland.

[10] Zanasi, R.; , "The Power-Oriented Graphs Technique: system modeling and basic properties", VPPC 2010, Lille, France, Sept. 2010.

[11] Zanasi, R.; Grossi, F.; Fei, M.; , "Complex Dynamic Models of Multi-phase Permanent Magnet Synchronous Motors", IFAC 2011, 18th IFAC World Congress, Milano, Italy, 28 Aug. - 2 Sept. 2011.

[12] Fei, M.; Zanasi, R.; , "Modeling of Multi Open Phase Fault Condition of Multi-phase Permanent Magnet Synchronous Motors", ACEMP and ELECTROMOTION 2011, Istanbul, Turkey, 08-10 Sept. 2011